Pergamon

Appl. Math. Lett. Vol. 8, No. 5, pp. 71–76, 1995

0893-9659/95 $9.50 + 0.00

0893-9659(95)00069-0

Explicit Solutions of a Simplified Model of Capillary Sprout Growth During Tumour Angiogenesis

H. M. BYRNE AND M. A. J. CHAPLAIN
School of Mathematical Sciences, University of Bath
Claverton Down, Bath BA2 7AY, U.K.

(Received February 1995; accepted March 1995)

Abstract—We present a mathematical model describing the growth and development of capillary sprouts in response to the chemotactic stimulus of a tumour angiogenesis factor (TAF). Exact analytical solutions are then derived for a simplified model which retain the salient qualitative features of the full model.

Keywords—Tumour angiogenesis, Chemotaxis, Nonlinear waves.

1. INTRODUCTION

Angiogenesis is crucial to the growth and development of solid tumours, forming a vital link between avascular and vascular tumour growth. Unless it is furnished with an adequate blood supply and a means, other than diffusion, of disposing of its waste products, a solid tumour cannot grow beyond a few millimetres in diameter and remains in an avascular state [1]. In order to escape from this dormant, avascular state, a solid tumour may secrete chemical compounds which stimulate any neighbouring endothelial cells (EC) into a well-ordered sequence of events [2]. Experiments performed using tumour implants in the cornea of test-animals [3] have enabled the detailed documentation of these events. The EC first secrete enzymes which degrade their basal lamina and they begin to migrate into the extracellular matrix. Small capillary sprouts are formed which grow towards the tumour by migration. Subsequently, EC close to the sprout tip undergo mitosis. Neighbouring capillaries fuse together to form closed loops (anastomoses) and from the primary loops, new capillary buds and sprouts emerge and a well-established capillary network is formed, which continues to advance towards the tumour eventually penetrating it. Vascularization of the tumour is achieved and vascular growth, with its insidious consequences of invasion and metastasis, may take place.

In this paper, we focus upon the migration of the capillary sprouts towards the tumour, developing and extending a continuum model of Balding and McElwain [4]. We assume unidirectional capillary sprout growth in the direction of the line connecting the tumour to the nearest site of EC (e.g., the limbus [3]) and we introduce dimensionless independent variables t and x to measure time and distance from the tumour (in contrast to [4], here the model is posed on a finite, rather than semi-infinite domain, with the tumour situated at $x = 0$, and the limbus at $x = 1$). The model equations describe interactions between the capillary sprout tip density (n), the vessel density within a sprout (ρ), and the chemottractant concentration, for example TAF, (c). The capillary tips move by random motion and also in response to the chemotactic gradient, are depleted by tip-to-branch collisions, that is anastomoses, and are produced by two differ-

ent mechanisms. The first mechanism describes branching behind the vascular front, with tips emanating from the capillary vessels and stimulated by the presence of TAF, whilst the second mechanism, which we term secondary proliferation, describes the rapid tip proliferation that occurs at the leading vascular edge [3], and is triggered by a threshold TAF concentration $\hat{c}$. The vessels within a sprout maintain a velocity which ensures continuity of the tip-vessel structure and decay linearly. The TAF concentration is governed by a simple reaction-diffusion equation, with linear decay. Specific features which distinguish our model from [4] are, then, the retention of random tip motility, the inclusion of a secondary tip proliferation rate, and a decay term for c. Experimental results [2], together with recent models [5,6] support the retention of μ whilst the inclusion of a secondary tip proliferation rate is designed to more accurately describe the experimentally observed brush-border effect [3]. Further, given the large number of angiogenic factors that may be secreted by a tumour, the second rate may be attributed to a different angiogenic factor. In summary, the model equations which we study are given by

$$\frac{\partial n}{\partial t} = \mu \frac{\partial^2 n}{\partial x^2} - \chi \frac{\partial}{\partial x}\left(n \frac{\partial c}{\partial x}\right) + \alpha_0 \rho c + \alpha_1 H(c - \hat{c}) n c - \beta n \rho, \tag{1}$$

$$\frac{\partial \rho}{\partial t} = \mu \frac{\partial n}{\partial x} - \chi n \frac{\partial c}{\partial x} - \gamma \rho, \tag{2}$$

$$\frac{\partial c}{\partial t} = \frac{\partial^2 c}{\partial x^2} - \lambda c, \tag{3}$$

where μ and χ describe the random tip motility and chemotaxis coefficients relative to the TAF diffusion coefficient; α_0 and α_1 are tip proliferation rates, the second rate acting only where a threshold TAF concentration $\hat{c}$ is exceeded; β is the rate of tip-to-branch anastomosis, and λ the rate of TAF decay. $H(.)$ is the usual Heaviside function. Boundary and initial conditions are now imposed to close the system. At the tumour, c is maintained at a constant value ($\equiv 1$, by suitable rescaling), and the tip density set to zero, in which case our model no longer applies once the tips penetrate the tumour. At the limbus, c is set to zero whilst n and ρ decay exponentially to zero and $\rho_{\min}$, at the rate k. The latter conditions are motivated by experimental results which suggest that, after their initial formation, capillary buds are no longer produced at the limbus. Continual recruitment of endothelial cells from the parent vessel, together with the physical constraint that $\rho(1,t) > 0$ which ensures sustained contact of the advancing vascular front with the parent vessel, motivates the decay of ρ to $\rho_{\min} > 0$ at $x = 1$. Initial TAF, tip and vessel densities, consistent with the boundary conditions, are prescribed. In summary, the following boundary and initial conditions are imposed (see [7] for further details):

$$n(0,t) = 0, \quad n(1,t) = n_L e^{-kt}, \quad n(x,0) = 0, \quad \text{for } 0 \le x < 1, \quad n(1,0) = n_L, \tag{4}$$

$$\rho(1,t) = \rho_{\min} + (1 - \rho_{\min}) e^{-kt}, \quad \rho(x,0) = 0, \quad \text{for } 0 \le x < 1, \quad \rho(1,0) = 1, \tag{5}$$

$$c(0,t) = 1, \quad (1,t) = 0, \quad c(x,0) = 0, \quad \text{for } 0 < x \le 1. \tag{6}$$

Numerical simulations of (1)–(6) illustrate that the balance between chemotaxis, tip proliferation and tip death affects the tumour's ability to secure a vascular network from the limbus. Typical simulations showing successful angiogenesis are presented in Figures 1a–b. In addition to reproducing the wavelike ingrowth of the vascular front obtained by Balding and McElwain (which correspond to $\alpha_0 = 50$, $\alpha_1 = 0$), we note that the simulations presented here capture several characteristics of capillary growth *not observed* in [4]. In particular, our model predicts both the increasing speed of the vascular front and the brush-border effect [3], with an increasingly developed vascular network evolving behind the leading capillary tip front, the resolution of these tip and vessel profiles a direct consequence of secondary tip proliferation. The sharp increase in the vessel density at $x = 1$ in Figure 1b arises from the prescription of ρ there (see equation (1)). However, we note from (2) that ρ satisfies an ODE in time at each value of x and that the boundary condition is superfluous. Its introduction is due solely to the requirements

of the numerical method employed. Finally, we note that simulations performed with $\alpha_0 = 0$, $\alpha_1 = 10$ are very similar to those of Figures 1a–b and would seem to justify the introduction of the autocatalytic term and the assumed key role of the threshold TAF concentration. Unsuccessful angiogenesis can also be modelled and typical simulations (cf. [7]) show both the tip and vessel density decaying away to zero throughout the domain before the tumour is reached.

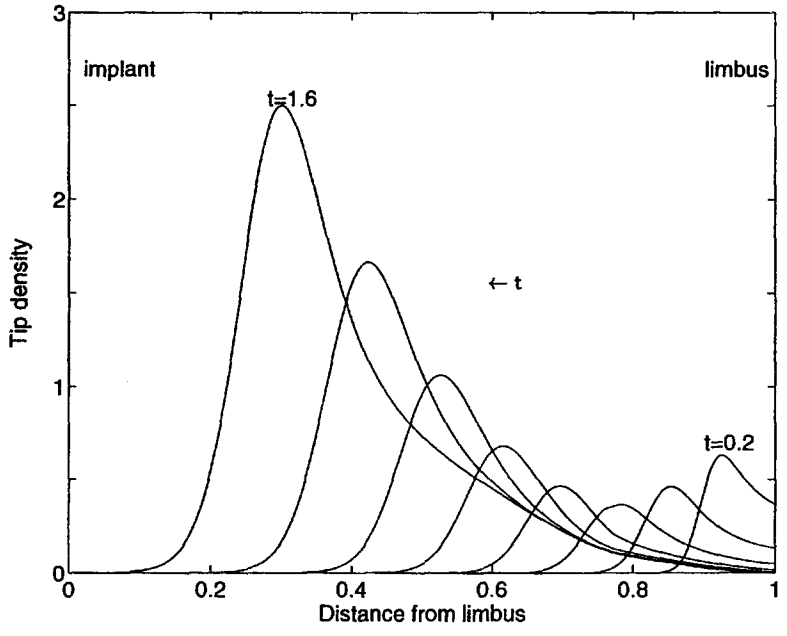

(a) Profile of the capillary tip density propagating from the limbus at $x = 1$ through the external host tissue to the tumour implant at $x = 0$. Secondary tip proliferation is included. Profiles are plotted at times $t = 0.2, 0.4, \ldots, 1.6$. Parameter values: $\alpha_0 = 50$, $\alpha_1 = 10$, $\beta = 50$, $\gamma = 0.25$, $\mu = 10^{-3}$, $\chi = 0.4$, $\lambda = 1$, $\hat{c} = 0.2$, $n_L = 1.0$, $k = 5.0$, $\rho_{\min} = 0.2$.

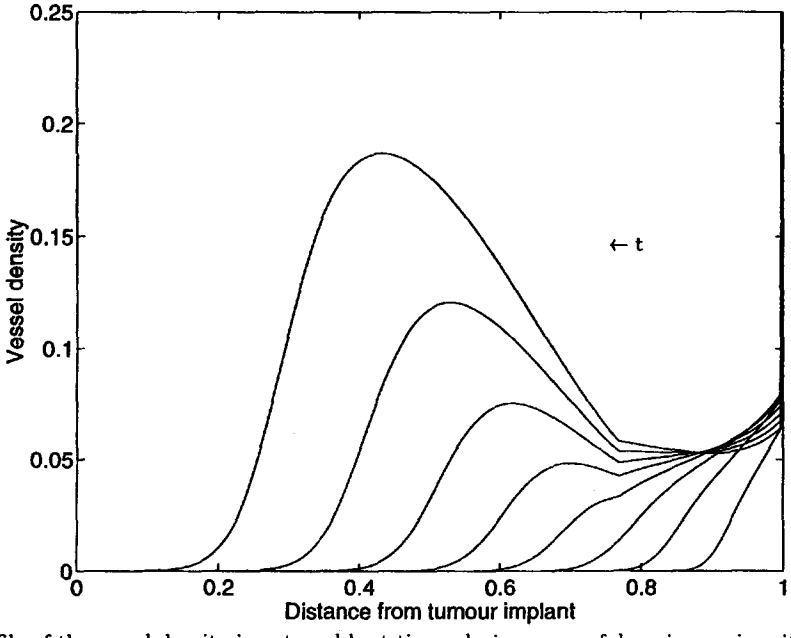

(b) Profile of the vessel density in external host tissue during successful angiogenesis, with parameter values as per Figure 1a.

Figure 1.

2. MODEL SIMPLIFICATION

In developing our simplified model, it is apparent from the numerical simulations (cf. [6,7]) that the TAF concentration c rapidly relaxes to a steady profile. (This observation is consistent with dimensional analysis of the system parameters which indicates that the attractant diffusion timescale is much shorter than the time taken for the vascular front to reach the tumour [7].) Simulations in [7] also indicate that incorporating an explicit coupling between the TAF concentration and the capillary tips (e.g., assuming the tips act as sinks for the TAF) does not significantly alter the results of the previous section. Thus, setting $\frac{\partial}{\partial t} = 0$ in (3) we obtain the following steady profile for c:

$$c(x) = \frac{\sinh\sqrt{\lambda}(1-x)}{\sinh\sqrt{\lambda}}. \tag{7}$$

Following Chaplain and Stuart [6], who estimated the motility coefficient for cells and chemicals $D_{\text{cell}}/D_{\text{chemical}} = \mu \sim 10^{-3}$, we fix $\mu = 0$ henceforth. Assuming further that the vessels respond instantaneously to changes in the tip density, we set $\frac{\partial}{\partial t} = 0$ in (2), so that ρ is defined in terms of n and c as follows:

$$\rho(x,t) = -\frac{\chi}{\gamma}\frac{dc}{dx}n = \left(\frac{\chi\sqrt{\lambda}\cosh\sqrt{\lambda}(1-x)}{\gamma\sinh\sqrt{\lambda}}\right)n(x,t), \tag{8}$$

and (1)–(1) reduce to the following nonlinear wave equation which defines $n(x,t)$:

$$\frac{\partial n}{\partial t} + \chi\frac{dc}{dx}\frac{\partial n}{\partial x} = \left\{\alpha_1 H(c-\hat{c}) - \chi\lambda - \frac{\alpha_0\chi}{\gamma}\frac{dc}{dx}\right\}cn + \frac{\beta\chi}{\gamma}\frac{dc}{dx}n^2 \equiv F(n,c), \tag{9}$$

subject to

$$n(0,t) = 0, \quad n(x,0) = H(x-x^*), \quad n(1,t) = 1,$$

for some $x^* \in (0,1)$. Our choice of initial data is based on the assumption that this caricature model is valid after transients associated with initiating the propagation of the vascular front and establishing a steady TAF profile have dissipated, by which time new capillary tips will occupy a finite region in a neighbourhood of the limbus, $[x^*,1]$ say.

From (8) and (9) we note that the wavespeed satisfies

$$\frac{dx}{dt} = \chi\frac{dc}{dx} = -\frac{\chi\sqrt{\lambda}\cosh\sqrt{\lambda}(1-x)}{\sinh\sqrt{\lambda}},$$

so that the vascular front propagates from the limbus ($x = 1$) to the tumour ($x = 0$) with increasing speed, a result qualitatively consistent with *in vivo* experimental measurements [8].

Explicit solutions of (9) may be constructed using the method of characteristics [9]. Using s to parametrise arc-length along a characteristic, we deduce from (8) and (9) that n and ρ satisfy

$$\frac{\partial n}{\partial s} \equiv \left(\frac{\partial}{\partial t} + \chi\frac{dc}{dx}\frac{\partial}{\partial x}\right)n = F(n,c),$$

$$\frac{\partial\rho}{\partial s} = -\frac{\chi}{\gamma}\frac{dc}{dx}\left(\frac{\partial n}{\partial s} + \chi n\frac{d^2c}{dx^2}\right).$$

With c defined by (7), we deduce further

$$\frac{\partial n}{\partial s} = 0 \Rightarrow \frac{\partial\rho}{\partial s} = -\frac{\chi^2}{\gamma}\frac{dc}{dx}\frac{d^2c}{dx^2}n > 0,$$

$$\frac{\partial\rho}{\partial s} = 0 \Rightarrow \frac{\partial n}{\partial s} = -\chi n\frac{d^2c}{dx^2} < 0.$$

Given that, for x fixed, s may be regarded as a timelike variable, the above result may be interpreted thus. When n attains its maximum value at a point, ρ is still increasing there.

Conversely, by the time that ρ attains its maximum at the same point in space, n is decreasing there. Thus our caricature model retains the qualitative features of the numerical simulations presented in Figure 1: as the vascular front advances towards the tumour the maximum tip density precedes the maximum vessel density, a result also consistent with experimental observations [3].

To further simplify the analysis, we make the following simplifying assumptions regarding the TAF concentration profile and the tip creation rates. The numerical simulations indicate that the concentration profile c does not vary greatly over the timescale under consideration and that in fact a very good (linear) approximation can be obtained by setting $c(x) = 1 - x$, in effect assuming $\lambda = 0$. Experimental evidence [2,3] indicates that tip creation at the leading vascular front dominates that behind, especially during the appearance of the "brush-border" effect [3], and so we also set $\alpha_0 = 0$. The vessel density is then directly proportional to the tip density ($\rho = \chi n/\gamma$), and (9) reduces to give

$$\frac{\partial n}{\partial t} - \chi \frac{\partial n}{\partial x} = \alpha_1 H(1 - x - \hat{c})(1 - x)n - \frac{\beta\chi}{\gamma} n^2. \tag{10}$$

With tip proliferation active only when $x \in (0, 1 - \hat{c})$ and the characteristics of (10) the family of straight lines $x + \chi t =$ constant, we remark that (x, t)-space may be partitioned into distinct regions according to the influence of the initial data and whether tip proliferation occurs there. Integrating along characteristics in the appropriate regions, the following expressions for the tip density may be obtained:

$$n_0(x,t) \equiv 0,$$
$$\text{in } 0 < x < x^*, \quad 0 < t < \frac{x^*}{\chi}, \quad t < \frac{(-x + x^*)}{\chi};$$
$$n_1(x,t) = \left(1 + \frac{\beta\chi t}{\gamma}\right)^{-1},$$
$$\text{in } x^* < x < 1, \quad \frac{(x^* - 1 + \hat{c})}{\chi} < t < \frac{\hat{c}}{\chi}, \quad \frac{(-x + x^*)}{\chi} < t < \frac{(-x + 1)}{\chi};$$
$$n_2(x,t) = \frac{n_1(1 - \hat{c}, t - (1 - \hat{c} - x)/\chi) \exp\{\alpha_1(1 - \hat{c} - x)(1 + \hat{c} - x)/2\chi\}}{1 + (\beta\chi/\gamma)\, n_1(1 - \hat{c}, t - (1 - \hat{c} - x)/\chi) \int_0^{(1-\hat{c}-x)/\chi} \exp\{\alpha_1\eta(\hat{c} + \chi\eta/2)\}\, d\eta},$$
$$\text{in } 0 < x < 1 - x^*, \quad \frac{(x^* - 1 + \hat{c})}{\chi} < t < \frac{\hat{c}}{\chi}, \quad \frac{(-x + x^*)}{\chi} < t < \frac{(-x + 1)}{\chi}.$$

The solution remains valid until $t = x^*/\chi$, at which time the characteristic passing through $(x, t) = (x^*, 0)$ reaches the tumour.

We now derive upper and lower bounds for n at $(0, x^*/\chi)$. Given that the initial tip density is normalised to unity, these bounds may be used to determine criteria under which angiogenesis succeeds (the lower bound exceeds unity) and under which angiogenesis fails (the upper bound is less than unity). Using the above expressions we deduce

$$n_{2L}\left(0, \frac{x^*}{\chi}\right) < n_2\left(0, \frac{x^*}{\chi}\right) < n_{2U}\left(0, \frac{x^*}{\chi}\right),$$

where

$$n_{2L}\left(0, \frac{x^*}{\chi}\right) = e^\theta \left(1 + \frac{\beta x^*}{\gamma} + \frac{\beta(1 - \hat{c})}{\gamma}\left(e^\theta - 1\right)\right)^{-1}, \quad n_{2U}\left(0, \frac{x^*}{\chi}\right) = e^\theta \left(1 + \frac{\beta x^*}{\gamma}\right)^{-1}.$$

and $\theta = \alpha_1(1 - \hat{c}^2)/2\chi$. We deduce that angiogenesis fails if $n_{2U}(0, x^*/\chi) < 1$, which, on rearrangement, yields the inequality

$$e^\theta = \exp\left\{\frac{\alpha_1}{2\chi}\left(1 - \hat{c}^2\right)\right\} < 1 + \frac{\beta x^*}{\gamma}.$$

Imposing $n_{2L}(0, x^*/\chi) > 1$ defines a second region of parameter space in which successful angiogenesis is predicted. Thus, the success or failure of angiogenesis is essentially governed by the balance between the proliferating parameter grouping α_1/χ and the 'death' parameters $\hat{c}, x^*$ and β/γ. For example, the parameter $\hat{c}$ denotes the threshold TAF concentration at which (secondary) tip proliferation is initiated. Given the steady TAF profile adopted here, increasing $\hat{c}$ reduces the size of the domain in which tip proliferation occurs, making angiogenesis less likely to occur. Increasing x^* has a similar effect whilst the appearance of the ratio α_1/χ may be explained thus. The greater the speed of the vascular front, the less time available for tip proliferation before the front reaches the tumour. Thus, the tip proliferation rate α_1 must be large enough, with respect to χ, to ensure that a well-developed vascular-front has been established during the time taken for the front to reach the tumour. The effect that increasing the parameter grouping β/γ has on diminishing the success of angiogenesis follows analogously.

3. CONCLUSIONS

We have developed a simple caricature model of capillary sprout growth during tumour angiogenesis which yields an explicit analytical solution and proved that it possesses a number of qualitative features which are consistent with experimental observations [3,8]. In addition, we were able to define the success (failure) of angiogenesis in terms of known parameters.

REFERENCES

1. R.M. Sutherland, Cell and environment interactions in tumor microregions: The multicell spheroid model, *Science* **240**, 177–184 (1988).
2. N. Paweletz and M. Knierim, Tumour-related angiogenesis, *Critical Reviews in Oncology/Hematology* **9**, 197–242 (1989).
3. V.R. Muthukkaruppan, L. Kubai and R. Auerbach, Tumour-induced neovascularization in the mouse eye, *J. Natl. Cancer Inst.* **69**, 699–705 (1982).
4. D. Balding and D.L.S. McElwain, A mathematical model of tumour-induced capillary growth, *J. Theor. Biol.* **114**, 53–73 (1985).
5. C.L. Stokes and D.A. Lauffenburger, Analysis of the roles of microvessel endothelial cell random motility and chemotaxis in angiogenesis, *J. Theor. Biol.* **152**, 377–403 (1991).
6. M.A.J. Chaplain and A.M. Stuart, A model mechanism for the chemotactic response of endothelial cells to tumour angiogenesis factor, *IMA J. Math. Appl. Med. Biol.* **10**, 149–168 (1993).
7. H.M. Byrne and M.A.J. Chaplain, Mathematical models for tumour angiogenesis: Numerical simulations and nonlinear wave solutions, *Bull. Math. Biol.* (in press) (1994).
8. J. Folkman, The vascularization of tumours, In *Cancer Biology: Readings from Scientific American*, (Edited by E.C. Friedberg), pp. 115–124, (1986).
9. W. Williams, *Partial Differential Equations*, Oxford University Press, (1980).